J. Am. Soc. Mass Spectrom. (2017) 28:2054–2065
DOI: 10.1007/s13361-017-1735-7

RESEARCH ARTICLE

Delivering Transmembrane Peptide Complexes to the Gas Phase Using Nanodiscs and Electrospray Ionization

Jun Li, Michele R. Richards, Elena N. Kitova, John S. Klassen

Alberta Glycomics Centre and Department of Chemistry, University of Alberta, Edmonton, T6G 2G2, Alberta, Canada

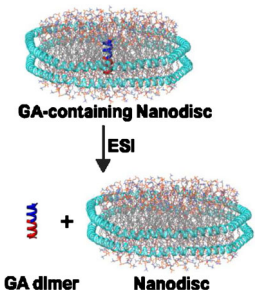

Abstract. The gas-phase conformations of dimers of the channel-forming membrane peptide gramicidin A (GA), produced from isobutanol or aqueous solutions of GA-containing nanodiscs (NDs), are investigated using electrospray ionization-ion mobility separation-mass spectrometry (ESI-IMS-MS) and molecular dynamics (MD) simulations. The IMS arrival times measured for $(2GA + 2Na)^{2+}$ ions from isobutanol reveal three different conformations, with collision cross-sections (Ω) of 683 $Å^2$ (conformation 1, C1), 708 $Å^2$ (C2), and 737 $Å^2$ (C3). The addition of $NH_4CH_3CO_2$ produced $(2GA + 2Na)^{2+}$ and $(2GA + H + Na)^{2+}$ ions, with Ω similar to those of C1, C2, and C3, as well as $(2GA + 2H)^{2+}$, $(2GA + 2NH_4)^{2+}$, and $(2GA + H + NH_4)^{2+}$ ions, which adopt a single conformation with a Ω similar to that of C2. These results suggest that the nature of the charging agents, imparted by the ESI process, can influence dimer conformation in the gas phase. Notably, the POPC NDs produced exclusively $(2GA + 2NH_4)^{2+}$ dimer ions; the DMPC NDs produced both $(2GA + 2H)^{2+}$ and $(2GA + 2NH_4)^{2+}$ dimer ions. While the Ω of $(2GA + 2H)^{2+}$ is similar to that of C2, the $(2GA + 2NH_4)^{2+}$ ions from NDs adopt a more compact structure, with a Ω of 656 $Å^2$. It is proposed that this compact structure corresponds to the ion conducting single stranded head-to-head helical GA dimer. These findings highlight the potential of NDs, combined with ESI, for transferring transmembrane peptide complexes directly from lipid bilayers to the gas phase.

Keywords: Electrospray ionization, Nanodiscs, Peptide complexes, Ion mobility separation, Collision cross-sections

Received: 18 April 2017/Revised: 25 May 2017/Accepted: 1 June 2017/Published Online: 5 July 2017

Introduction

Membrane peptides and proteins are implicated in many critical cellular processes, including signal transduction, transport, and metabolism [1, 2]. Although their biological significance is well-established, the structural and functional analysis of membrane proteins and peptides and their complexes in a native lipid bilayer environment remains experimentally challenging. Commonly used approaches involve the incorporation of the peptide/protein into model membranes (e.g., micelles, bicelles, lipid bilayers, and vesicles) [3–6] or detergent systems [7], which provide both a native-like membrane environment and allow for integration with conventional structural and biophysical techniques. Nanodiscs (NDs), which are water-soluble discoidal phospholipid bilayers surrounded by two copies of an amphipathic membrane scaffold protein (MSP), represent a popular alternative to present membrane peptides and proteins [8, 9]. NDs, combined with diverse structural and biophysical techniques, including X-ray crystallography and nuclear magnetic resonance (NMR), optical and surface plasmon resonance (SPR) spectroscopies, as well as electrochemistry [9–13], have been used to probe the properties of isolated membrane proteins and peptides, as well as their complexes with other proteins, peptides, and lipids. Recently, electrospray ionization-mass spectrometry (ESI-MS), implemented with NDs, has emerged as a promising tool for studying the binding properties of membrane peptides and proteins in a lipid environment [14–16]. Moreover, collision cross-sections (Ω), measured using ion mobility separation (IMS), provides a means of assessing possible conformations of the gaseous peptide/protein ions produced from the NDs [17]. However, the extent to which the structures of the gaseous ions reflect the conformations present in the membrane remains unclear, in particular for small peptide complexes, for which

Electronic supplementary material The online version of this article (doi:10.1007/s13361-017-1735-7) contains supplementary material, which is available to authorized users.

Correspondence to: John Klassen; *e-mail:* john.klassen@ualberta.ca

electrostatic effects may influence conformation in the gas phase.

Here, we describe the application of ESI-MS and IMS to investigate the conformations of the gas-phase ions of dimers of the transmembrane peptide gramicidin A (GA) produced from NDs. Homodimers of GA are known to act as monovalent cation-selective channels in membranes [18]. Owing to its small size and ready availability (from the soil bacteria *Bacillus brevis*), GA has been extensively used as a model to study the organization, dynamics, and function of transmembrane peptide channels [19, 20]. The GA peptide (HCO-Val-Gly-Ala-D-Leu-Ala-D-Val-Val-D-Val-Trp-D-Leu-Trp-D-Leu-Trp-D-Leu-Trp-$NHCH_2CH_2OH$) consists of aliphatic and aromatic amino acids, with a protected N-terminus (formylated) and C-terminus (ethanolamide). The alternating L- and D-amino acids sequence causes the peptides to adopt β-helical conformers, with the side chains projecting out from the exterior surface of the helix formed by the peptide backbone [18]. The distribution of monomeric and dimeric GA, as well as the dimer conformations, are strongly influenced by environment. In polar solvents, such as dimethyl sulfoxide, GA exists predominantly as monomer [21]. In alcohols, GA forms parallel and antiparallel double-stranded double helix (DSDHp and DSDHap, respectively) dimers, and the extent of GA dimerization varies from ~5% to ~85% (with dimerization increasing with increasing hydrophobicity) [22–24]. The DSDH dimers are stabilized by intermolecular H-bonds between backbone amide groups [18]. When incorporated into lipid membranes, GA forms monovalent cation channels. The results of electrophysiological experiments performed on the GA ion channel in lipid bilayers suggest that there is single ion conducting structure [18]. Based on solution NMR spectroscopy data measured for GA-containing micelles and high-resolution solid-state NMR data acquired for GA dimers in a lipid bilayer, it has been proposed that the antiparallel single stranded head-to-head helical (SSHH) dimer is the ion conducting form of GA [25, 26]. The SSHH structure is formed by transmembrane dimerization, stabilized by intermolecular H-bonds between the two N-termini, of two nearly cylindrical monomers residing in opposite leaflets with their axes aligned to form a channel across the bilayer. The four Trp residues in the C-termini are positioned such that they can form H-bonds to polar residues at the bilayer/solution interface [19].

Recently, ESI-IMS-MS was used to probe the conformations of gaseous GA dimer ions produced using the phospholipid vesicle capture-freeze-drying (VCFD) method [27, 28]. Briefly, vesicles containing GA are freeze-dried and then resuspended in isobutanol for ESI-IMS-MS analysis [27, 28]. Three different conformations of the gaseous GA dimers, detected as $(2GA + 2Na)^{2+}$ ions, were identified from phospholipid vesicles sprayed out of isobutanol; these were assigned as DSDHp, DSDHap, and SSHH based on a comparison of the Ω measured for these ions and values calculated from molecular dynamics (MD) simulations carried out on structures measured using X-ray crystallography and NMR spectroscopy [27]. It was later reported that the nature of the phospholipid and the presence of cholesterol influences the relative abundances of the three conformations [28]. Implementation of the VCFD method using a mixing tee ESI setup, which allows fast mixing between aqueous vesicles and organic solvent and reduces sample preparation time, was also recently described [29]. Although relatively straightforward to implement, a potential weakness of the VCFD method is that the original conformation(s) of the peptide dimer in the phospholipid bilayer may be altered prior to the IMS measurements due to exposure to isobutanol.

In the present study, the conformations of GA dimer ions produced by ESI performed on aqueous solutions of GA-containing NDs composed of 1,2-dimyristoyl-sn-glycero-3-phosphocholine (DMPC) or 1-palmitoyl-2-oleoyl-*sn*-glycero-3-phosphocholine (POPC) were analyzed by ESI-IMS-MS and the measured Ω compared with those obtained using the VCFD method. Measurements were also performed on GA dimer ions produced from isobutanol solutions to probe whether the conformations present in the gas phase exhibit any dependence on the nature of the ESI charging agents. The Ω determined experimentally for the gaseous GA dimer ions were compared with values calculated for structures obtained by X-ray and NMR spectroscopy and from MD simulations.

Experimental

Proteins, Peptides, and Lipids

Gramicidin A (GA, ≥90% purity, MW 1882.33 Da) was purchased from Sigma-Aldrich Canada (Oakville, Canada) and used without further purification. As described below, the GA sample also contained gramicidin B (GB, HCO-Val-Gly-Ala-D-Leu-Ala-D-Val-Val-D-Val-Trp-D-Leu-Phe-D-Leu-Trp-D-Leu-Trp-$NHCH_2CH_2OH$, MW 1843.30 Da) as an impurity. Recombinant membrane scaffold protein (MSP1E1, MW 27,494 Da) was expressed and purified as previously described [8]. Cytochrome *c* from equine heart (cyt *c*, MW 12,384 Da), myoglobin from equine heart (myo, MW 16,951 Da), which were used to construct the Ω calibration curve for IMS measurements, were purchased from Sigma-Aldrich Canada. The phospholipids DMPC (MW 677.9 Da) and POPC (MW 760.08 Da) were purchased from Avanti Polar Lipids Inc. (Alabaster, AL, USA). The structures of the phospholipids are shown in Figure S1, Supporting Information.

Nanodisc Preparation

Nanodiscs were prepared according to a protocol reported previously [8, 9]. Briefly, DMPC or POPC (dissolved in chloroform) was mixed with GA (dissolved in ethanol) in the desired ratio (160:1 molar ratio of phospholipid-to-GA). The lipid and peptide mixture was dried under N_2 and kept in a vacuum desiccator overnight at room temperature to form a lipid film, and then resuspended in 20 mM TrisHCl, 0.5 mM EDTA, 100 mM NaCl, 25 mM sodium cholate (pH 7.4), and sonicated for 15 min. MSP1E1 was added at 1:100 molar ratio

of MSP1E1-to-total lipid followed by incubation for 15 min. ND formation was initiated by adding an equal volume of Bio-Beads (Bio-Rad Laboratories Ltd., Mississauga, Canada), and the solution was incubated at room temperature for 3 h for DMPC ND and at 4 °C for 4 h for POPC ND to remove all detergent. Finally, the GA-containing NDs were purified using a Superdex 200 10/300 size exclusion column (GE Healthcare Bio-Sciences, Uppsala, Sweden), which was equilibrated in 200 mM ammonium acetate (pH 6.8). The corresponding size exclusion chromatograms are shown in Figure S2 (Supporting Information) [30]. The ND concentration was calculated based on the MSP1E1 concentration, which was measured by UV absorbance at 280 nm and using an extinction coefficient of 32 430 M^{-1} cm^{-1}. The purified NDs were concentrated using a 30 kDa MW cut-off filter, to approximately 30 µM, and stored at –80 °C until needed.

Mass Spectrometry

All MS measurements were performed in positive ion mode using a Synapt G2S quadrupole-ion mobility separation-time-of-flight (Q-IMS-TOF) mass spectrometer (Waters, Manchester, UK) equipped with nanoflow ESI (nanoESI) sources. Borosilicate capillaries (1.0 mm o.d., 0.68 mm i.d.) were pulled in-house using a P-1000 micropipette puller (Sutter Instruments, Novato, CA, USA). A voltage of ~1.0 kV applied to a platinum wire was inserted into the nanoESI tip and a source temperature of 60 °C and a cone voltage 50 V were used. Argon was used in the Trap and Transfer ion guides at pressures of 2.77×10^{-2} mbar and 2.84×10^{-2} mbar, respectively, and the Trap and Transfer voltages were 5 V and 2 V, respectively. To dissociate GA dimers, the *m/z* region corresponding to GA dimer ions was selected by quadrupole mass filter and the ions subjected to collision-induced dissociation (CID) in Transfer region following IMS, at voltages ranging from 2 V to 50 V. For IMS, a wave height of 38 V and a wave velocity of 800 m s^{-1} were applied, and the helium and nitrogen gas flow rates were 190 mL min^{-1} and 60 mL min^{-1}, respectively. The Ω of the GA dimer ions were determined from the IMS measurements using a protocol described previously [31, 32]. Briefly, IMS arrival time (ATs) were converted to Ω using a calibration plot constructed from ATs, measured under identical instrumental conditions, for calibrant ions with known Ω (Figure S3, Supporting Information). Doubly protonated tryptic peptides obtained from cytochrome *c* and myoglobin with known Ω (in He) served as the calibrant ions (Table S1, Supporting Information) [33, 34]. All data was processed using the Waters MassLynx software (ver. 4.1) in combination with Driftscope ver. 2.5. Gaussian functions, fit using the multipeak fitting function of Igor pro 6.22A, were used to describe the IMS arrival time distributions (ATDs) and the fitting was evaluated from an analysis of the residuals.

Molecular Dynamics (MD) Simulations

Molecular dynamics simulations were performed on GA dimer ions charged with two Na^+ or two NH_4^+ cations. A total of 12 different GA dimer ion structures were investigated. The starting structures were based on reported structures for DSDHp, DSHHap, and SSHH GA dimers. For the DSDHp GA dimer, two models (models 1 and 4) taken from the NMR spectroscopy results reported by Chen et al. were used (PDB ID: 1MIC, Figure S4, Supporting Information) [35]; for the DSDHap GA dimer, two different X-ray structures – one crystalized from ethanol (PDB ID: 1ALZ, Figure S5, Supporting Information) [36] and another in complex with CsCl (PDB ID: 1AV2, Figure S5, Supporting Information) [37] – were used; for the SSHH GA dimer, two different NMR spectroscopy structures – one with GA in a DMPC bilayer (PDB ID: 1MAG, Figure S6, Supporting Information) [38] and another with GA in a DDPC micelle with excess Na^+ present (PDB ID: 1NRU, Figure S6, Supporting Information) [39] – were used. For all the simulations performed on GA dimers charged with Na^+, except the ones involving 1AV2, the cations were added using the *addIons* command in the *tleap* module of AmberTools15 [40]. For the 1AV2 structure, the two Cs^+ ions associated with chain A in the PDB file were replaced with either Na^+. For the simulations performed on GA dimers charged with NH_4^+, the Na^+ ions were replaced with the nitrogen atom of NH_4^+ ions, and the hydrogens were added using the *tleap* module of AmberTools15 [40].

All simulations were run in the gas phase using the *sander* module in AMBER12 [41]. The *ff14SB* force field [42] was used for both the L- and D-amino acids, as well as for NH_4^+ ions, and Joung-Cheatham parameters were used for Na^+ [43]. Partial charges for the N-terminal formyl group, the C-terminal ethanolamine, and the NH_4^+ ion were assigned using the AM1 with bond charge correction (AM1-BCC) model [44] in the *antechamber* module of AmberTools15 [40]. The systems were first minimized using 5000 steps of steepest decent, followed by 5000 steps of conjugate gradient. The systems were heated from 5 K to 300 K over 100 ps, and then allowed to run at 300 K for 100 ps before the 500 ns production simulations were started. The timestep was 2 fs, bonds to hydrogen were constrained with the SHAKE [45] algorithm, and the cutoff for non-bonded interactions was infinite (999.0 Å). The temperature was maintained with the Berendsen thermostat [46] (*ntt* = 1) with velocities rescaled every 1 ps.

Theoretical Collision Cross-Sections

Theoretical Ω values were calculated for GA dimer structures produced over the course of the MD simulations using the MOBCAL trajectory method [47, 48]. Fifty structures were chosen from the 500 ns production simulation, one structure every 10 ns, and the Ω values were calculated with the MOBCAL software parameter *imp* set to 50. Theoretical Ω values were also calculated for GA dimer structures taken directly from Protein Data Bank (PDB) [49]. For DSDHap GA dimer, structures 1AL4, 1ALX, 1ALZ were used [36, 37], for DSDHp GA dimer, the 10 models in 1MIC were used [35], and for SSHH GA dimer, structures 1JNO, 1MAG, 1NRM, and 1NRU were used [38, 39, 50, 51]. Because each

PDB structure was a single set of coordinates, the Ω values were calculated with the MOBCAL software parameter *imp* set to 1000.

Results and Discussion

GA Dimer Ions Produced from Isobutanol

Prior to investigating the conformations of gaseous GA dimers produced from NDs, ESI-IMS-MS was used to analyze isobutanol solutions of GA. Shown in Figure S7a (Supporting Information) is a representative mass spectrum acquired for an isobutanol solution of 5 μM GA (equilibrated for 48 h at 25 °C). The major species detected were the sodiated adducts of the GA monomer and homodimer, i.e., $(GA + 2Na)^{2+}$ (*m/z* 963.54, based on monoisotopic mass), and $(GA + Na)^{+}$ and $(2GA + 2Na)^{2+}$ (*m/z* 1904.08) ions. Also detected were ions corresponding to the sodiated adducts of the heterodimer of GA and GB, i.e., $(GA + GB + 2Na)^{2+}$ (*m/z* 1884.56), and the mixed sodium and potassium adducts of the GA homodimer, i.e., $(2GA + Na + K)^{2+}$ (*m/z* 1912.07).

A plot of IMS arrival time (ATs) measured for *m/z* 1904.08 ions (and the corresponding isotopomers) revealed two features (Figure S7b, Supporting Information). The dominant feature, attributed to $(2GA + 2Na)^{2+}$ ions, exhibited three distinct (but only partially resolved) arrival time distributions (ATDs), with ATs centered at 10.82 ms (referred to as conformation 1, C1), 11.38 ms (conformation 2, C2), and 12.20 ms (conformation 3, C3), and a lower abundance feature, centered at 15.74 ms, corresponding to $(GA + Na)^{+}$ ions. The mass spectra corresponding to each of these ATs are shown in Figure S7c–7f (Supporting Information), along with the expected theoretical isotopomer distributions calculated for the $(2GA + 2Na)^{2+}$ and $(GA + Na)^{+}$ ions (Figure S7g–7h, Supporting Information). The full width at half maximum (FWHM) for the deconvoluted ATDs (represented as Gaussian functions) for the three $(2GA + 2Na)^{2+}$ conformations are relatively small, 0.44 ms (C1), 0.50 ms (C2), and 0.31 ms (C3), consistent with the presence of three well-defined dimer conformations. In contrast, the broad feature observed for the $(GA + Na)^{+}$ ions (FWHM 1.3 ms) is suggestive of ions with significant conformational flexibility. This finding is consistent with reported results obtained from MD simulations [52]. The IMS-AT data measured for the $(2GA + Na + K)^{2+}$ ions (*m/z* 1912.07) is also suggestive of three distinct conformations, with ATDs centered at 10.92 ms, 11.53 ms, and 12.40 ms (Figure S7j, Supporting Information). In contrast, the IMS-AT data for $(GA + GB + 2Na)^{2+}$ (*m/z* 1884.56) consists of a single broad feature (FWHM 0.95 ms) centered at 11.05 ms (Figure S7o, Supporting Information), which suggests the presence of multiple, but structurally-similar, conformations. A single IMS-ATD, centered at 4.95 ms (FWHM of 0.34), was measured for $(GA + 2Na)^{2+}$ (*m/z* 963.54) (Figure S7r, Supporting Information).

The IMS-ATs measured for the GA monomer and dimer ions were converted to Ω (in He) using the calibration plot constructed from the tryptic peptide calibrant ions (Figure S3, Supporting Information) [33, 34]. Using this calibration approach, the Ω of the three conformations of $(2GA + 2Na)^{2+}$ were found to be 683 Å^2 (C1), 708 Å^2 (C2), and 737 Å^2 (C3), respectively (Table 1). These values agree, within 2%, with values reported previously by Russell and co-workers [53]. Similar Ω were also found for the three conformations of $(2GA + Na + K)^{2+}$ ions (688 Å^2, 714 Å^2, and 749 Å^2, Table 1), suggesting that the $(2GA + Na + K)^{2+}$ ions adopt the same C1, C2, and C3 conformations. The Ω for the $(GA + GB + 2Na)^{2+}$ ions, based on the averaged IMS-AT, is 694 Å^2 (Table 1). This value is somewhat less than the weighted average of the C1, C2, and C3 values, suggesting that the replacement of Trp (GA) with Phe (GB) influences dimer conformation in isobutanol.

The ESI-IMS-MS data, taken on their own, suggest that ~59% of GA exists as dimer in isobutanol. This value is in good agreement with a value of ~55% determined previously by ESI-MS [53]. However, given the possibility that the GA monomer and dimer have different ionization and detection efficiencies (i.e., ESI-MS response factors), the distribution of GA monomer and dimer present in solution may not be quantitatively reflected in the ESI-MS data. Similarly, assuming that the multiple conformations detected for the $(2GA + 2Na)^{2+}$ and $(2GA + Na + K)^{2+}$ ions are reflective of solution structures and that they have uniform response factors, the ESI-MS data suggest that the GA homodimer exists in three distinct conformations (i.e., C1, C2, and C3) in isobutanol, with relative abundances of 30%, 68%, and 2%, respectively. These results are in reasonable agreement with the distribution of $(2GA + 2Na)^{2+}$ conformers reported previously (36%, 61%, and 3%) [53].

GA Dimer Ions Produced from Isobutanol Saturated with Ammonium Acetate

To investigate whether charging in the ESI process affects the conformations of gaseous GA dimer ions detected from isobutanol, the measurements were repeated using solutions containing ammonium acetate. Shown in Figure S8a (Supporting Information) is a representative mass spectrum acquired for GA (5 μM) in isobutanol (equilibrated for 48 h at 25 °C) saturated with ammonium acetate. In addition to the $(2GA + 2Na)^{2+}$, $(GA + Na)^{+}$, and $(GA + 2Na)^{2+}$ ions, the mass spectrum revealed signal corresponding to $(2GA + 2H)^{2+}$ and $(GA + H)^{+}$ (*m/z* 1882.11), $(2GA + H + NH_4)^{2+}$ (*m/z* 1890.63), $(2GA + H + Na)^{2+}$ (*m/z* 1893.11), $(2GA + 2NH_4)^{2+}$ and $(GA + NH_4)^{+}$) (*m/z* 1899.15), $(GA + 2H)^{2+}$ (*m/z* 941.57), and $(GA + 2Na)^{2+}$ ions (*m/z* 952.57). The IMS-AT data measured for $(2GA + 2Na)^{2+}$ are similar to those described above; the Ω for the three conformations (690 Å^2, 714 Å^2, and 746 Å^2, Table 1) are within 2% of values measured in the absence of ammonium acetate (Figure S8b, Supporting Information). This result, on its own, suggests that the presence of ammonium acetate ions does not perturb the GA dimer structures in isobutanol. Three conformations were also detected for the

Table 1. Ion Mobility Separation Arrival Times (IMS-ATs) and Corresponding Collision Cross-Sections (Ω, in He) Measured for GA Dimer and Monomer Ions Produced by ESI from Isobutanol Solutions (With and Without Ammonium Acetate) and Aqueous Ammonium Acetate Solutions of GA-Containing NDs

Solvent	GA ions	*m/z*	Arrival time (ms)	FWHM (ms)	Ω (Å^2)
Isobutanol	$(2GA+2Na)^{2+}$	1904.08	10.82	0.44	683
			11.38	0.50	708
			12.20	0.31	737
	$(GA+GB+2Na)^{2+}$	1884.56	11.05	0.95	694
	$(2GA+Na+K)^{2+}$	1912.07	10.92	0.52	688
			11.53	0.78	714
			12.40	0.38	749
	$(GA+Na)^{+}$	1904.08	15.74	1.30	441
	$(GA+2Na)^{2+}$	963.54	4.95	0.34	407
Isobutanol	$(2GA+2H)^{2+}$	1882.11	11.45	0.60	711
saturated $NH_4CH_3CO_2$	$(2GA+H+NH_4)^{2+}$	1890.63	11.55	0.56	715
	$(2GA+H+Na)^{2+}$	1893.11	11.19	0.44	700
			11.63	0.41	718
			12.07	0.43	736
	$(2GA+2NH_4)^{2+}$	1899.15	11.55	0.64	715
	$(2GA+2Na)^{2+}$	1904.08	10.95	0.40	690
			11.52	0.67	714
			12.32	0.31	746
	$(GA+H)^{+}$	1882.11	15.31	0.81	434
	$(GA+NH_4)^{+}$	1899.15	14.50	0.75	419
	$(GA+Na)^{+}$	1904.08	15.65	1.18	441
	$(GA+2H)^{2+}$	941.57	4.94	0.23	408
	$(GA+H+Na)^{2+}$	952.57	4.95	0.25	407
	$(GA+2Na)^{2+}$	963.54	4.95	0.27	407
Aqueous $NH_4CH_3CO_2$ solution of GA-containing DMPC ND	$(2GA+2NH_4)^{2+}$	1899.15	10.15	0.43	656
	$(2GA+2H)^{2+}$	1882.11	11.44	0.56	710
	$(GA+NH_4)^{+}$	1899.15	14.96	0.73	428
	$(GA+H)^{+}$	1882.11	15.68	0.83	442
	$(GA+2H)^{2+}$	941.57	4.95	0.23	408
Aqueous $NH_4CH_3CO_2$ solution of GA-containing POPC ND	$(2GA+2NH_4)^{2+}$	1899.15	10.15	0.48	656
	$(GA+NH_4)^{+}$	1899.15	14.77	1.67	425
	$(GA+H)^{+}$	1882.11	16.05	0.72	448
	$(GA+2H)^{2+}$	941.57	4.95	0.32	408

$(2GA + H + Na)^{2+}$ ions, with Ω (700 Å^2, 718 Å^2, and 736 Å^2, Table 1) similar to those of the $(2GA + 2Na)^{2+}$ ions (Figure S8y, Supporting Information). In contrast, the IMS-AT data acquired for the $(2GA + 2H)^{2+}$, $(2GA + H + NH_4)^{2+}$, and $(2GA + 2NH_4)^{2+}$ ions are suggestive of a single conformation in the gas phase (Figures S8j, S8o, and S8v, Supporting Information), with Ω values (711 Å^2, 715 Å^2, and 715 Å^2, respectively, Table 1), similar to that of C2. The IMS-AT data measured for the $(GA + H)^+$ and $(GA + NH_4)^+$ ions give Ω in the range of 419 Å^2 to 434 Å^2, which is slightly less than that of $(GA + Na)^+$. Likewise, the Ω measured for the $(GA + 2H)^{2+}$ and $(GA + H + Na)^{2+}$ ions (407 Å^2 and 408 Å^2, respectively, Table 1) are indistinguishable from that of $(GA + 2Na)^{2+}$.

Taken together, the IMS results obtained for the GA ions produced from isobutanol solutions, alone or with ammonium acetate, provide experimental evidence that the nature of the ESI charging agent can influence the conformations of GA dimer ions detected in the gas phase. Despite being produced from the same solution, three distinct conformations were observed for GA dimer ions charged by one or two Na^+, but only a single conformation for GA dimer ions charged by H^+ or NH_4^+. While the origin of these structural differences could not be conclusively established, vide infra, they presumably arise from differences in the nature of the interactions between the different charging agents with the peptides. As described in more detail below, the results of MD simulations performed on desolvated, doubly charged GA dimers revealed that both Na^+ and NH_4^+ are solvated predominantly by carbonyl oxygens, although the average number of interactions is significantly different for the two cations. Regardless of the exact origin of the conformational differences in the GA dimer ions, the present findings highlight a potential complication in using IMS-derived Ω as a probe of the conformations of peptide complexes in solution.

GA Dimer Ions Produced from NDs

According to available structural data, the GA dimer exists preferentially in the SSHH form when present in a lipid bilayer, and the DSDHp and DSDHap forms when present in organic solvents [22, 23, 25, 26]. Consequently, it was of interest to probe the Ω of gas-phase GA dimer ions produced directly from ND lipid bilayers in aqueous solution and to compare them to values measured for dimer ions produced from isobutanol. Shown in Figures 1 and 2 are representative ESI mass spectra and corresponding IMS data acquired for an aqueous ammonium acetate (200 mM, pH 6.8) solution of GA-containing DMPC ND (Figure 1) or GA-containing POPC ND (Figure 2). In both cases, the major species detected correspond to protonated DMPC or POPC ions. For the DMPC

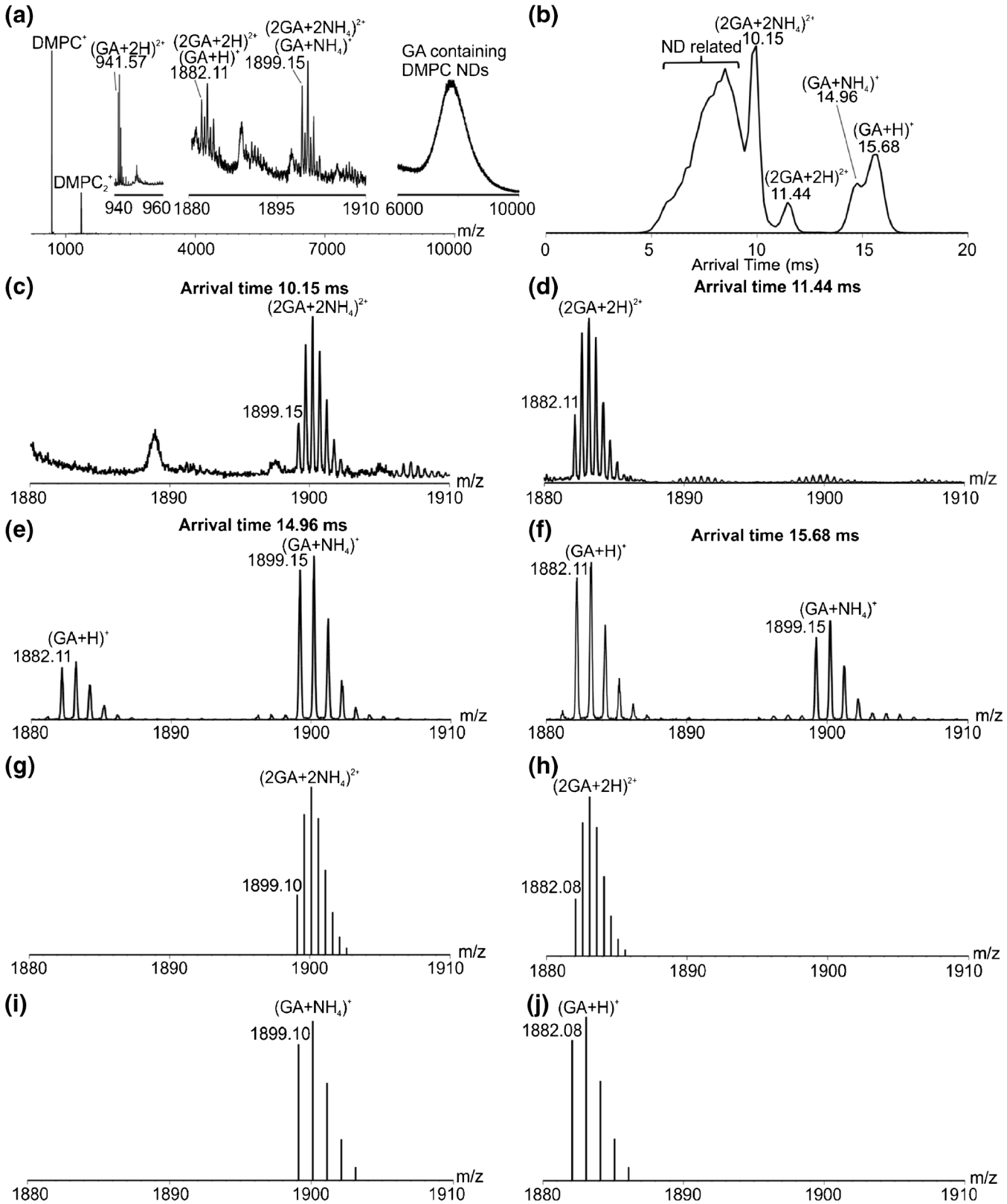

Figure 1. (**a**) ESI mass spectrum acquired for aqueous ammonium acetate solution (200 mM, pH 6.8, 25 °C) of GA-containing DMPC NDs (15 μM); (**b**) Plot of IMS-ATs measured for all ions between *m/z* 1880 and *m/z* 1910; (**c**) and (**d**) ESI mass spectra corresponding to IMS-AT 10.15 ms and 11.44 ms, respectively; (**e**) and (**f**) ESI mass spectra corresponding to AT 14.96 ms and 15.68 ms, respectively; (**g**), (**h**), (**i**), and (**j**) theoretical isotopic distributions for $(2GA + 2NH_4)^{2+}$, $(2GA + 2H)^{2+}$, $(GA + NH_4)^{+}$, and $(GA + H)^{+}$, respectively

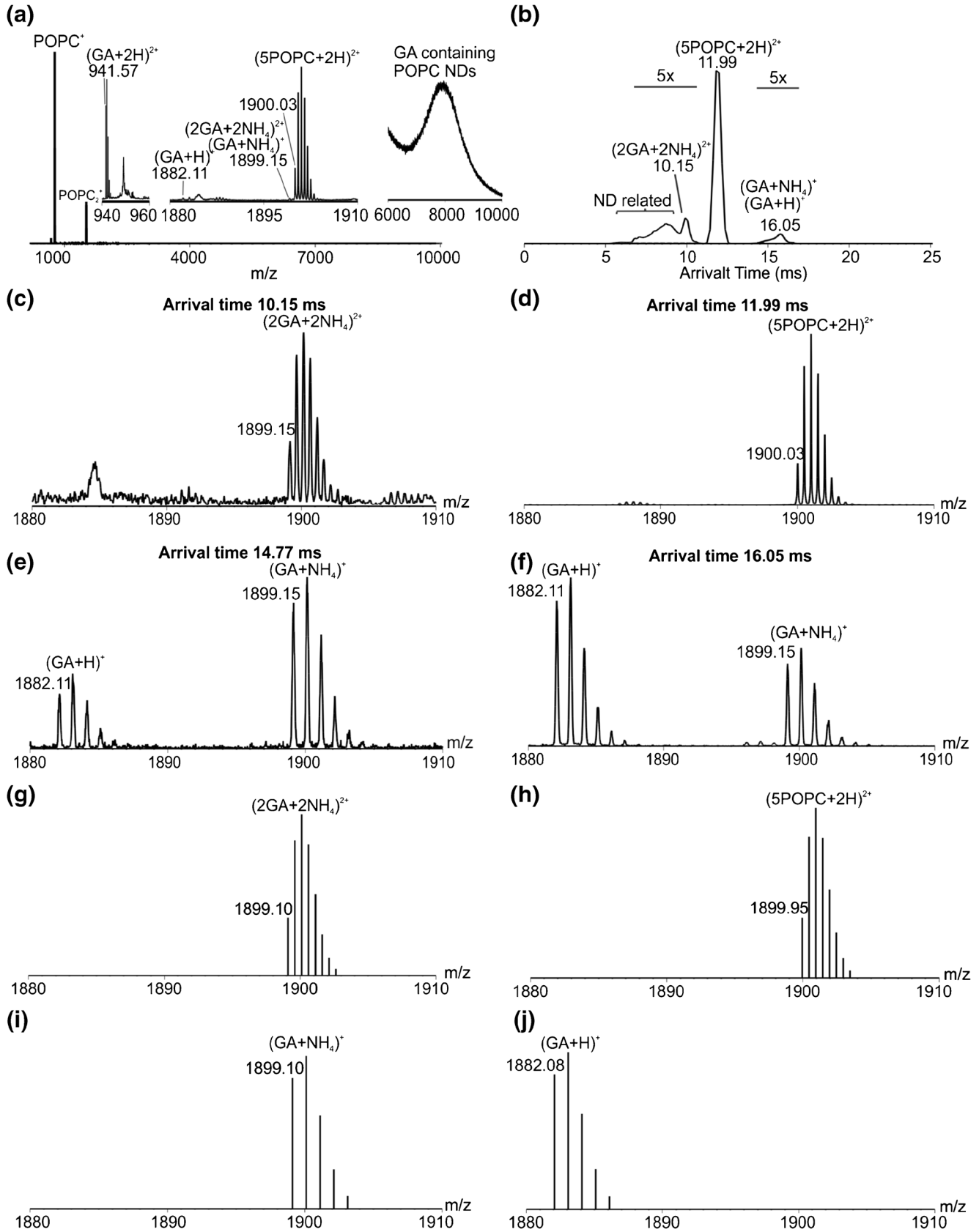

Figure 2. (**a**) ESI mass spectrum acquired for aqueous ammonium acetate solution (200 mM, pH 6.8, 25 °C) of GA-containing POPC NDs (15 μM); (**b**) plot of IMS-ATs measured for all ions between *m/z* 1880 and *m/z* 1910; (**c**), (**d**), (**e**), and (**f**) ESI mass spectra corresponding to IMS-AT 10.15 ms, 11.99 ms, 14.77 ms, and 16.05 ms, respectively; (**g**), (**h**), (**i**), and (**j**) theoretical isotopic distributions for $(2GA + 2NH_4)^{2+}$, $(5POPC + 2H)^{2+}$, $(GA + NH_4)^{+}$, and $(GA + H)^{+}$, respectively

NDs, the GA dimer ions, $(2GA + 2H)^{2+}$ and $(2GA + 2NH_4)^{2+}$, were detected, along with monomeric species, $(GA + H)^+$, $(GA + NH_4)^+$, and $(GA + 2H)^{2+}$ (Figure 1). It is proposed that the GA dimers are spontaneously ejected from the NDs upon transfer to the gas phase in a process that is analogous to what has been previously reported in ESI-MS studies of protein–glycolipid complexes involving water soluble lectins and glycolipids incorporated into NDs [30]. The broad feature centered at *m/z* ~8000 is attributed to intact ND ions [54]. Collisional activation of these ions (at *m/z* ≥6000) in the Trap region (20 V) resulted in the appearance of $(GA + NH_4)^+$ monomer ions, indicating the incomplete release of GA from the NDs in the source (Figure S9, Supporting Information). For the POPC NDs, only the $(2GA + 2NH_4)^{2+}$ dimer ion were detected; monomeric $(GA + H)^+$ ions and $(GA + NH_4)^+$ ions were also produced (Figure 2). Similar to what was observed for the DMPC ND ions, collisional activation of the POPC ND ions (at *m/z* ≥6000) in the Trap region (20 V) resulted in the appearance of $(GA + NH_4)^+$ monomer ions (Figure S10, Supporting Information).

The Ω measured for the monomeric GA ions, $(GA + H)^+$, $(GA + NH_4)^+$, and $(GA + 2H)^{2+}$, (442 Å^2, 428 Å^2, 408 Å^2, respectively, Table 1), as well as the $(2GA + 2H)^{2+}$ dimer ion (710 Å^2, Table 1), produced from DMPC NDs, are similar to the values measured for these ions produced from the isobutanol solution containing ammonium acetate. In contrast, the Ω measured for the $(2GA + 2NH_4)^{2+}$ ions (656 Å^2, Table 1) is significantly less than that measured for the $(2GA + 2NH_4)^{2+}$ ions produced from isobutanol (715 Å^2, Table 1). Similar findings were obtained from the IMS analysis of the GA-containing POPC NDs. The results indicate that the GA dimer present in the NDs exist predominantly in a conformation (referred to here as C4) that is distinct from those adopted in isobutanol. Furthermore, given that this conformation was only observed when GA was present in a lipid bilayer, it may be further speculated that C4 originates from the native, ion conducting SSHH form of GA. The observation of a compact GA dimer produced from NDs contrasts with recent results, obtained using the VCFD method, where the same three conformations (with Ω of 673 Å^2, 697 Å^2, and 725 Å^2, respectively) were detected for $(2GA + 2Na)^{2+}$ ions from DMPC and POPC vesicles [27]. Although the reason behind these differences is not fully understood, these results show that the nature of the method used to deliver the GA dimers from a lipid bilayer to the gas phase can influence the conformation(s) of the gaseous ions.

It is also curious that the $(2GA + 2NH_4)^{2+}$ and $(2GA + 2H)^{2+}$ ions produced from the DMPC NDs exhibit significantly different Ω. This observation has at least two possible explanations – there are two GA dimer conformers present in the DMPC NDs or the larger $(2GA + 2H)^{2+}$ ions originate from the loss of NH_3 from the more compact $(2GA + 2NH_4)^{2+}$ ions. To test the latter, CID was performed on the $(2GA + 2NH_4)^{2+}$ ions in the Transfer region at voltages ranging from 2 V to 50 V (Figure 3). It can be seen that the $(2GA + 2NH_4)^{2+}$ ions dissociate preferentially into $(GA + NH_4)^+$ ions, which in turn

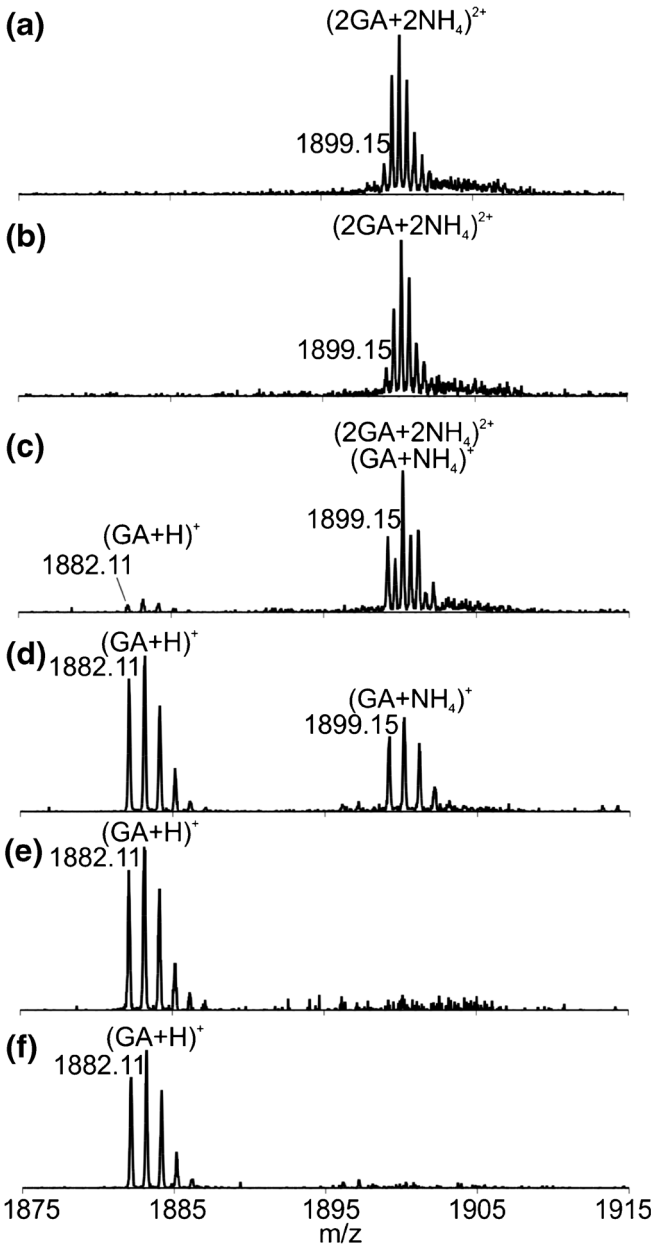

Figure 3. CID mass spectra acquired in the Transfer region for $(2GA + 2NH_4)^{2+}$, produced from aqueous ammonium acetate solution (200 mM, pH 6.8, 25 °C) of GA-containing DMPC NDs (15 μM), at voltages of (**a**) 2 V, (**b**) 10 V, (**c**) 20 V, (**d**) 30 V, (**e**) 40 V, and (**f**) 50 V

convert to give $(GA + H)^+$ ions; there is no evidence of $(2GA + 2H)^{2+}$ ion formation. This result, together with the absence of $(2GA + 2H)^{2+}$ ion produced from the POPC NDs, suggests that there are two different GA dimer structures in the solutions of DMPC ND, but only one dominant structure in the POPC ND solution.

Additional, albeit indirect, insights into the differences in GA dimer structures in the ND solutions can be found from the results obtained when sodium acetate was added to the aqueous ammonium acetate solutions of GA-containing NDs (Figures S11 and S12, Supporting Information). Notably, $(2GA + H + Na)^{2+}$ and $(2GA + 2Na)^{2+}$ ions were produced, in addition

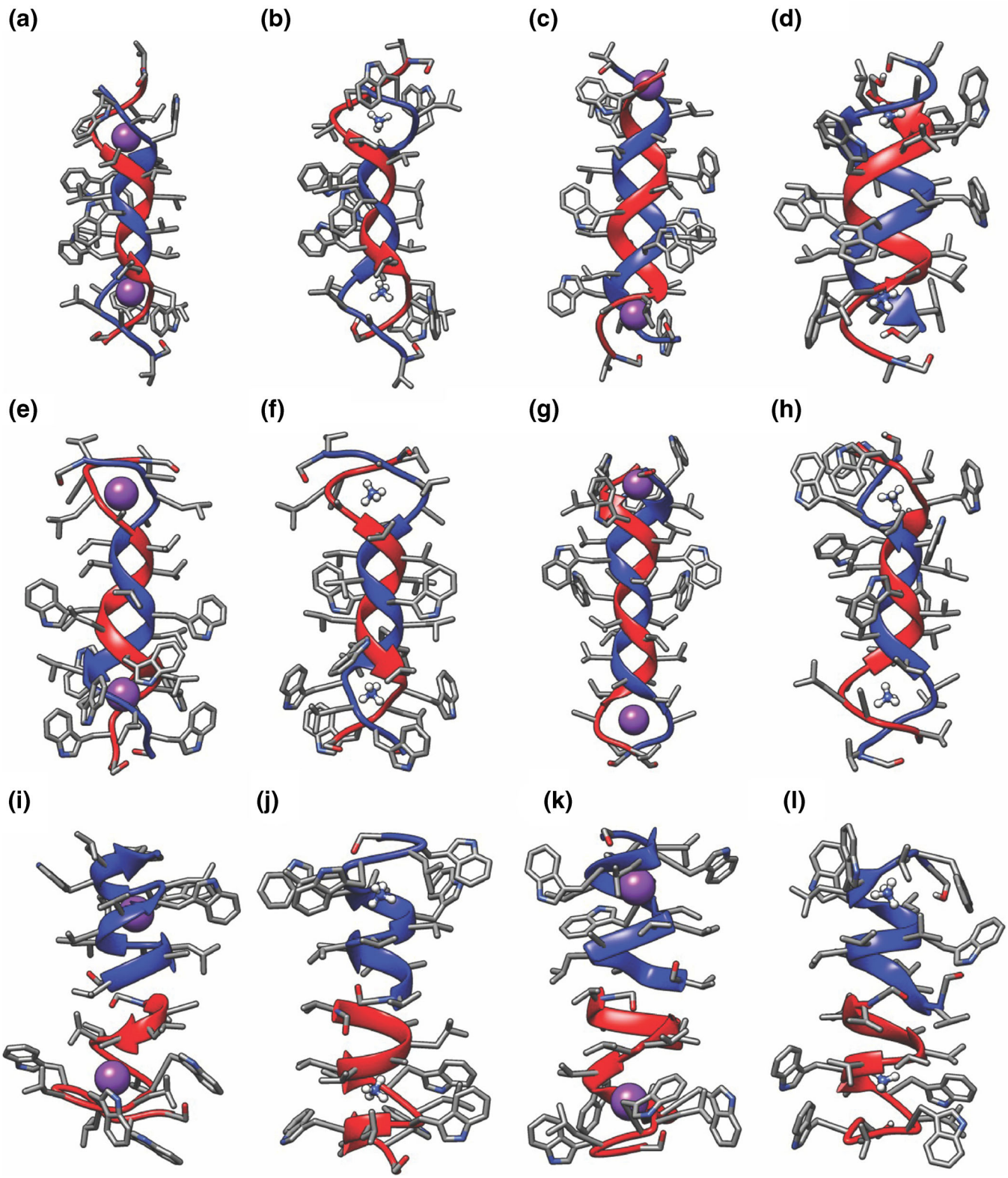

Figure 4. Average structures of the DSDHap form of GA dimer from MD simulations: (**a**) 1ALZ with 2 Na^+; (**b**) 1ALZ with 2 NH_4^+; (**c**) 1AV2 with 2 Na^+; (**d**) 1AV2 with 2 NH_4^+. Average structures of the DSDHp form of GA dimer from MD simulations: (**e**) 1MIC, model 1, with 2 Na^+; (**f**) 1MIC, model 1, with 2 NH_4^+; (**g**) 1MIC, model 4, with 2 Na^+; (**h**) 1MIC, model 4, with 2 NH_4^+. Average structures of the SSHH form of GA dimer from MD simulations: (**i**) 1MAG with 2 Na^+; (**j**) 1MAG with 2 NH_4^+; (**k**) 1MAG with 2 Na^+; (**l**) 1MAG with 2 NH_4^+

to $(2GA + 2H)^{2+}$ and $(2GA + 2NH_4)^{2+}$ ions, from the DMPC NDs. The Ω of the $(2GA + H + Na)^{2+}$ and $(2GA + 2Na)^{2+}$ ions (710 $Å^2$) are indistinguishable from the value measured for $(2GA + 2H)^{2+}$ (Figure S11, Supporting Information). In contrast, no Na^+ adducts of GA dimers were detected for the POPC NDs (Figure S12, Supporting Information); however, $(GA + Na)^+$ ions were observed. Taken together, these results suggest that the mechanism of ESI charging of the compact GA dimer (i.e., $(2GA + 2NH_4)^{2+}$) is distinct from that of GA monomer ions and $(2GA + 2H)^{2+}$ produced from the ND solutions. One possible explanation is that the GA dimer exists in the ion conducting SSHH form in the ND bilayer and is associated with NH_4^+ cations, present at high concentration in solution, which are retained in the gas phase. An alternative explanation would see the compact GA dimer ionized, post-transfer of the ND to the gas phase. In this case, ESI charging of the dimer will reflect the available charging agents associated with the gaseous ND ions. If the ESI droplets and, correspondingly, the NDs are primarily charged by NH_4^+ ions, these will be the main charging agents for the GA ions released from the NDs. According to the proposed models, the less compact GA dimer exists either in a structure that does not bind cations in solution or is more "exposed" to the charging agents in the ESI droplets.

Computational Results

Motivated by the observation of the compact $(2GA + 2NH_4)^{2+}$ ions produced from the NDs, a series of MD simulations were carried out on $(2GA + 2Na)^{2+}$ and $(2GA + 2NH_4)^{2+}$ ions and their Ω calculated at various timepoints along the trajectory. As described in the Experimental section, 500 ns simulations were performed using two different initial structures, taken from the PDB, for each the three helical classes of GA dimer [49].

Analysis of the MD results revealed that the overall helical structure of each ion was preserved throughout the simulations. The length of the helices, as measured along the helical axis, exhibited modest fluctuations that were independent of charging agent, with values ranging from 2.5 nm to 3.2 nm (DSDHp), 2.4 nm to 3.0 nm (DSDHap), and 1.6 nm to 3.2 nm (SSHH). It was also found that regardless of initial placement, the charging agents ended up in the interior of the helix (Figure 4). Both the Na^+ and NH_4^+ cations interact preferentially with backbone carbonyl oxygens; the Na^+ ions were almost fully solvated, with an average of 5.8 interactions per ion over the simulation, while each NH_4^+ participated, on average, in 2.7 H-bonds.

The Ω calculated for the $(2GA + 2Na)^{2+}$ and $(2GA + 2NH_4)^{2+}$ ions over the course of the simulation for each helical class (Figure 5) were found to span a significant and overlapping range of values, 616 to 690 $Å^2$ (DSDHp), 590 to 688 $Å^2$ (DSDHap), and 616 to 702 $Å^2$ (SSHH). The average Ω values are listed in Table S2 (Supporting Information). Interestingly, the nature of the charging agent did not have any significant effect on the Ω values. Moreover, the calculated Ω are similar in magnitude to the Ω values measured for C4 and C1, but consistently less than those corresponding to C2 and C3. Finally, it is notable that the Ω values determined from the MD simulations are reasonably similar in magnitude to the theoretical Ω values calculated for 17 different GA dimer structures taken from the PDB (613–658 $Å^2$ (DSDHp), 642–680 $Å^2$ (DSDHap), and 641–654 $Å^2$ (SSHH) (Figure 5).

Two significant findings emerge from this analysis. First, the structures of the GA dimers, regardless of conformation (i.e., DSDHp, DSDHap or SSHH), span a wide range of

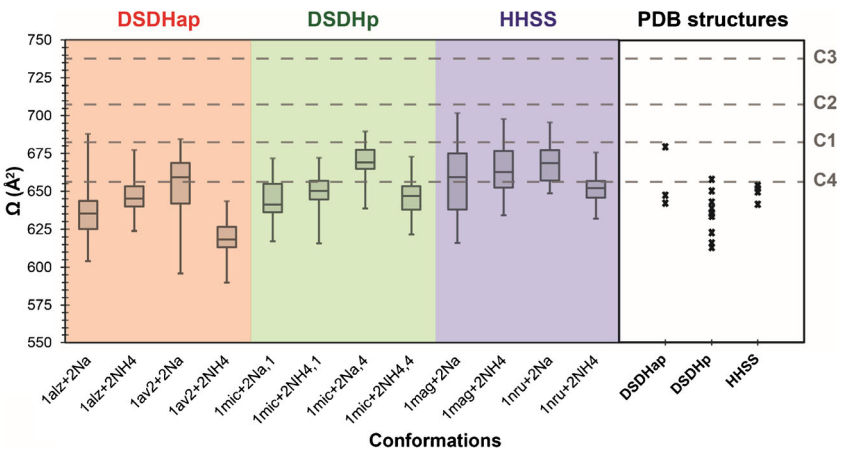

Figure 5. Ω calculated using the MOBCAL trajectory method for GA dimer structures taken from the Protein Data Bank (PDB) and structures generated from MD simulations. The Ω values calculated for the structures from MD simulations are shown as box plots, in which the error bars represent the entire range of Ω values, the boxes show the 25th–75th percentile, and the interior line represents the median value. The Ω values calculated for the structures from the PDB are represented by an X in the plot. For the DSDHap GA dimer, the PDB structures used are 1AL4, 1ALX, and 1ALZ; for the DSDHp GA dimer, the PDB structures used are the 10 models in 1MIC; and for SSHH GA dimer the PDB structures used are 1JNO, 1MAG, 1NRM, and 1NRU. The Ω values for C1 (683 $Å^2$), C2 (708 $Å^2$), C3 (737 $Å^2$), and C4 (656 $Å^2$) are shown as dashed horizontal lines

overlapping Ω values. Second, these Ω values are consistently lower than the experimental values measured for C2 and C3. Consequently, it would seem that it is not possible to unambiguously infer dimer conformation from a comparison of the Ω measured for the gaseous ions and values calculated from structures available in the PDB or from MD simulations (as performed in the present study). That the measured Ω of C2 and C3 are consistently higher than the calculated values raises the possibility that the helices are partially disordered in the gas phase. Indeed, the structures of the C2 and C3 conformations of the $(2GA + 2Na)^{2+}$ ions proposed by Russell and coworkers exhibit some fraying of the helices, suggestive of partial unfolding of the peptides, which could be caused by collisional heating of the gaseous ions [28, 55].

Conclusions

The results of the present study provide useful insights into the application of ESI-IMS-MS to probe the influence of solvent environment on the conformations of membrane peptide complexes. Importantly, it is found that the transmembrane GA dimer is readily transferred from phospholipid NDs to the gas phase by ESI. However, the Ω values measured for GA dimers produced from NDs differ from those determined for DMPC or POPC vesicles using the VCFD method [27]. Although the origin of these conformational differences is not fully understood and requires further investigation, this finding suggests that the method used to deliver the peptide complexes from the lipid bilayer to the gas phase may influence the conformations of the gaseous ions. Moreover, the results acquired for GA dimer ions produced from solutions of isobutanol with and without ammonium acetate, suggest that the nature of the charging agents imparted by the ESI process can influence dimer conformation in the gas phase, potentially complicating the structural interpretation of measured Ω values.

Acknowledgements

The authors are grateful for financial support provided by the National Sciences and Research Council of Canada and the Alberta Glycomics Centre.

References

1. Nath, A., Atkins, W.M., Sligar, S.G.: Applications of phospholipid bilayer nanodiscs in the study of membranes and membrane proteins. Biochemistry **46**, 2059–2069 (2007)
2. Denisov, I.G., Sligar, S.G.: Nanodiscs for structural and functional studies of membrane proteins. Nat. Struct. Mol. Biol. **23**, 481–486 (2016)
3. Sanders, C.R., Prosser, R.S.: Bicelles: a model membrane system for all seasons? Structure **6**, 1227–1234 (1998)
4. Sanders, C.R., Landis, G.C.: Reconstitution of membrane proteins into lipid-rich bilayered mixed micelles for NMR studies. Biochemistry **34**, 4030–4040 (1995)
5. Kashara, M., Hinkle, P.C.: Reconstitution and purification of D-glucose transporter from human erythrocytes. J. Biol. Chem. **252**, 7384–7390 (1977)
6. Rigaud, J.L., Paternostre, M.T., Bluzat, A.: Mechanisms of membrane protein insertion into liposomes during reconstitution procedures involving the use of detergents. 2. Incorporation of the light-driven proton pump bacteriorhodopsin. Biochemistry **27**, 2677–2688 (1988)
7. Seddon, A.M., Curnow, P., Booth, P.J.: Membrane proteins, lipids and detergents: not just a soap opera. Biochim. Biophys. Acta **1666**, 105–117 (2004)
8. Bayburt, T.H., Grinkova, Y.V., Sligar, S.G.: Self-assembly of discoidal phospholipid bilayer nanoparticles with membrane scaffold proteins. Nano Lett. **2**, 853–856 (2002)
9. Bayburt, T.H., Sligar, S.G.: Membrane protein assembly into nanodiscs. FEBS Lett. **584**, 1721–1727 (2010)
10. Hagn, F., Etzkorn, M., Raschle, T., Wagner, G.: Optimized phospholipid bilayer nanodiscs facilitate high-resolution structure determination of membrane proteins. J. Am. Chem. Soc. **135**, 1919–1925 (2013)
11. Wang, X., Mu, Z., Li, Y., Bi, Y., Wang, Y.: Smaller nanodiscs are suitable for studying protein lipid interactions by solution NMR. Protein J. **34**, 205–211 (2015)
12. Ritchie, T.K., Kwon, H., Atkins, W.M.: Conformational analysis of human ATP-binding cassette transporter ABCB1 in lipid nanodiscs and inhibition by the antibodies MRK16 and UIC2. J. Biol. Chem. **286**, 39489–39496 (2011)
13. Mak, P.J., Gregory, M.C., Denisov, I.G., Sligar, S.G., Kincaid, J.R.: Unveiling the crucial intermediates in androgen production. Proc. Natl. Acad. Sci. U. S. A. **112**, 15856–15861 (2015)
14. Hopper, J.T., Yu, Y.T., Li, D., Raymond, A., Bostock, M., Liko, I., Mikhailov, V., Laganowsky, A., Benesch, J.L., Caffrey, M., Nietlispach, D., Robinson, C.V.: Detergent-free mass spectrometry of membrane protein complexes. Nat. Methods **10**, 1206–1208 (2013)
15. Hebling, C.M., Morgan, C.R., Stafford, D.W., Jorgenson, J.W., Rand, K.D., Engen, J.R.: Conformational analysis of membrane proteins in phospholipid bilayer nanodiscs by hydrogen exchange mass spectrometry. Anal. Chem. **82**, 5415–5419 (2010)
16. Marty, M.T., Hoi, K.K., Gault, J., Robinson, C.V.: Probing the lipid annular belt by gas-phase dissociation of membrane proteins in nanodiscs. Angew. Chem. Int. Ed. **55**, 550–554 (2016)
17. Bernstein, S.L., Dupuis, N.F., Lazo, N.D., Wyttenbach, T., Condron, M.M., Bitan, G., Teplow, D.B., Shea, J.E., Ruotolo, B.T., Robinson, C.V., Bowers, M.T.: Amyloid-β protein oligomerization and the importance of tetramers and dodecamers in the etiology of Alzheimer's disease. Nat. Chem. **1**, 326–331 (2009)
18. Andersen, O.S., Koeppe II, R.E., Roux, B.: Gramicidin channels. IEEE Trans. NanoBiosci. **4**, 10–20 (2005)
19. Kelkar, D.A., Chattopadhyay, A.: The gramicidin ion channel: a model membrane protein. Biochim. Biophys. Acta Biomembr. **1768**, 2011–2025 (2007)
20. Miloshevsky, G.V., Jordan, P.C.: Permeation in ion channels: the interplay of structure and theory. Trends Neurosci. **27**, 308–314 (2004)
21. Veatch, W.R., Blout, E.R.: The aggregation of gramicidin A in solution. Biochemistry **13**, 5257–5264 (1974)
22. Veatch, W.R., Fossel, E.T., Blout, E.R.: The conformation of gramicidin A. Biochemistry **13**, 5249–5256 (1974)
23. Bystrov, V.F., Arseniev, A.S.: Diversity of the gramicidin A spatial structure: two-dimensional ^{1}H NMR study in solution. Tetrahedron **44**, 925–940 (1988)
24. Braco, L., Bano, C., Chillaron, F., Abad, C.: Dimer-monomer conformational equilibrium of gramicidin A in 1-alkanols as studied by HPLC and fluorescence spectroscopy. Int. J. Biol. Macromol. **10**, 343–348 (1988)
25. Arseniev, A.S., Barsukov, I.L., Bystrov, V.F., Lomize, A.L., Ovchinnikov, Y.A.: 1H-NMR study of gramicidin A transmembrane ion channel. Head-to-head right-handed, single stranded helices. FEBS Lett. **186**, 168–174 (1985)
26. Ketchem, R.R., Hu, W., Cross, T.A.: High-resolution conformation of gramicidin A in a lipid bilayer by solid-state NMR. Science **261**, 1457–1460 (1993)
27. Patrick, J.W., Gamez, R.C., Russell, D.H.: Elucidation of conformer preferences for a hydrophobic antimicrobial peptide by vesicle capture-freeze-drying: a preparatory method coupled to ion mobility-mass spectrometry. Anal. Chem. **87**, 578–583 (2015)
28. Patrick, J.W., Gamez, R.C., Russell, D.H.: The influence of lipid bilayer physicochemical properties on gramicidin A conformer preferences. Biophys. J. **110**, 1826–1835 (2016)

29. Patrick, J.W., Zerfas, B., Gao, J., Russell, D.H.: Rapid capillary mixing experiments for the analysis of hydrophobic membrane complexes directly from aqueous lipid bilayer solutions. Analyst **142**, 310–315 (2017)
30. Leney, A.C., Fan, X., Kitova, E.K., Klassen, J.S.: Nanodiscs and electrospray ionization mass spectrometry. A novel tool for screening glycolipids against proteins. Anal. Chem. **86**, 5271–5277 (2014)
31. Ruotolo, B.T., Benesch, J.L.P., Sandercock, A.M., Hyung, S.J., Robinson, C.V.: Ion mobility-mass spectrometry analysis of large protein complexes. Nat. Protoc. **3**, 1139–1152 (2008)
32. Bush, M.F., Hall, Z., Giles, K., Hoyes, J., Robinson, C.V., Ruotolo, B.T.: Collision cross-sections of proteins and their complexes: a calibration framework and database for gas-phase structural biology. Anal. Chem. **82**, 9557–9565 (2010)
33. Hoaglund, C.S., Valentine, S.J., Sporleder, C.R., Reily, J.P., Clemmer, D.E.: Three-dimensional ion mobility/TOFMS analysis of electrosprayed biomolecules. Anal. Chem. **70**, 2236–2242 (1998)
34. Henderson, S.C., Valentine, S.J., Counterman, A.E., Clemmer, D.E.: ESI/ion trap/ion mobility/time-of-flight mass spectrometry for rapid and sensitive analysis of biomolecular mixtures. Anal. Chem. **71**, 291–301 (1999)
35. Chen, Y., Tucker, A., Wallace, B.A.: Solution structure of a parallel left-handed double-helical gramicidin-A determined by 2D 1H NMR. J. Mol. Biol. **264**, 757–769 (1996)
36. Burkhart, B.M., Gassman, R.M., Langs, D.A., Pangborn, W.A., Duax, W.L.: Heterodimer formation and crystal nucleation of gramicidin D. Biophys. J. **75**, 2135–2146 (1998)
37. Burkhart, B.M., Li, N., Langs, D.A., Pangborn, W.A., Duax, W.L.: The conducting form of gramicidin A is a right-handed double-stranded double helix. Proc. Natl. Acad. Sci. U. S. A. **95**, 12950–12955 (1998)
38. Ketchem, R.R., Lee, K.-C., Huo, S., Cross, T.A.: Macromolecular structural elucidation with solid-state NMR-derived orientational constraints. J. Biomol. NMR **8**, 1–14 (1996)
39. Townsley, L.E.: Gramicidin A in dodecyl phosphocholine micelles in the presence of excess Na^+. (PDB ID: 1NRU) (2003)
40. Case, D.A., Berryman, J.T., Betz, R.M., Cerutti, D.S., Cheatham, T.E. III, Darden, T.A., Duke, R.E., Giese, T.J., Gohlke, H., Goetz, A.W., Homeyer, N., Izadi, S., Janowski, P., Kaus, J., Kovalenko, A., Lee, T.S., LeGrand, S., Li, P., Luchko, T., Luo, R., Madej, B., Merz, K.M., Monard, G., Needham, P., Nguyen, H., Nguyen, H.T., Omelyan, I., Onufriev, A., Roe, D.R., Roitberg, A., Salomon-Ferrer, R., Simmerling, C.L., Smith, W., Swails, J., Walker, R.C., Wang, J., Wolf, R.M., Wu, X., York, D.M., Kollman, P.A.: AMBER 15, University of California: San Francisco, CA (2015)
41. Case, D.A., Darden, T.A., Cheatham, T.E. III, Simmerling, C.L., Wang, J., Duke, R.E., Luo, R., Walker, R.C., Zhang, W., Merz, K.M., Roberts, B., Hayik, S., Roitberg, A., Seabra, G., Swails, J., Götz, A.W., Kolossváry, I., Wong, K.F., Paesani, F., Vanicek, J., Wolf, R.M., Liu, J., Wu, X., Brozell, S.R., Steinbrecher, T., Gohlke, H., Cai, Q., Ye, X., Wang, J., Hsieh, M.-J., Cui, G., Roe, D.R., Mathews, D.H., Seetin, M.G., Salomon-Ferrer, R., Sagui, C., Babin, V., Luchko, T., Gusarov, S., Kovalenko, A., Kollman, P.A.: AMBER 12, University of California: San Fancisco, CA (2012)
42. Hornak, V., Abel, R., Okur, A., Strockbine, B., Roitberg, A., Simmerling, C.: Comparison of multiple Amber force fields and development of improved protein backbone parameters. Proteins **65**, 712–725 (2006)
43. Joung, I.S., Cheatham, T.E.: Determination of alkali and halide monovalent ion parameters for use in explicitly solvated biomolecular simulations. J. Phys. Chem. B **112**, 9020–9041 (2008)
44. Jakalian, A., Bush, B.L., Jack, D.B., Bayly, C.I.: Fast, efficient generation of high-quality atomic charges. AM1-BCC model: I. Method. J. Comput. Chem. **21**, 132–146 (2000)
45. Ryckaert, J.-P., Ciccotti, G., Berendsen, H.J.C.: Numerical integration of the Cartesian equations of motion of a system with constraints: molecular dynamics of n-alkanes. J. Comput. Phys. **23**, 327–341 (1977)
46. Berendsen, H.J.C., Postma, J.P.M., Gunsteren, W.F.V., DiNola, A., Haak, J.R.: Molecular dynamics with coupling to an external bath. J. Chem. Phys. **81**, 3684–3690 (1984)
47. Shvartsburg, A.A., Jarrold, M.F.: An exact hard-spheres scattering model for the mobilities of polyatomic ions. Chem. Phys. Lett. **261**, 86–91 (1996)
48. Mesleh, M.F., Hunter, J.M., Shvartsburg, A.A., Schatz, G.C., Jarrold, M.F.: Structural information from ion mobility measurements: effects of the long-range potential. J. Phys. Chem. **100**, 16082–16086 (1996)
49. RSCB Protein Data Bank. Available at: www.rcsb.org. Accessed 14 March 2017
50. Townsley, L.E., Tucker, W.A., Sham, S., Hinton, J.F.: Structures of gramicidin A, B, and C incorporated into sodium dodecyl sulfate micelles. Biochemistry **40**, 11676–11686 (2001)
51. Townsley, L..: Gramicidin A in dodecyl phosphocholine micelles. (PDB ID: 1NRM). (2003)
52. Chen, L., Gao, Y.Q., Russell, D.H.: How alkali metal ion binding alters the conformation preferences of gramicidin A: a molecular dynamics and ion mobility study. J. Phys. Chem. A **116**, 689–696 (2012)
53. Chen, L., Chen, S.H., Russell, D.H.: An experimental study of the solvent-dependent self-assembly/disassembly and conformer preferences of gramicidin A. Anal. Chem. **85**, 7826–7833 (2013)
54. Zhang, Y., Liu, L., Daneshfar, R., Kitova, E.N., Li, C., Jia, F., Cairo, C.W., Klassen, J.S.: Protein–glycosphingolipid interactions revealed using catch-and-release mass spectrometry. Anal. Chem. **84**, 7618–7621 (2012)
55. Chen, L.: Gas-phase and solution-phase peptide conformations studied by ion mobility-mass spectrometry and molecular dynamics simulations. Ph.D. thesis, Texas A&M University, College Station, TX (2012)